

Force sensing with an optically levitated charged nanoparticle

David Hempston, Jamie Vovrosh, Marko Toroš, Muddassar Rashid,* and Hendrik Ulbricht†
Department of Physics and Astronomy, University of Southampton, SO17 1BJ, United Kingdom
 (Dated: May 18, 2022)

Levitated optomechanics is showing potential for precise force measurements. Here, we report a case study, to show experimentally the capacity of such a force sensor. Using an electric field as a tool to detect an applied Coulomb force on levitated nanosphere. We experimentally study the spatial displacement, of up to 7.1 nm, on the levitated nanosphere by imposing a DC field. We further apply an AC field and demonstrate resonant enhancement of force sensing when a driving frequency, ω_{AC} , and the natural frequency of the levitated mechanical oscillator, ω_0 , converge. We directly measure a force of $3.0 \pm 1.5 \times 10^{-20}$ N with 10 second integration, at room temperature and at a pressure of 1.6×10^{-5} mbar.

The ability to detect forces with increasing sensitivity, is of paramount importance for many fields of studies, from detecting gravitational waves [1] to molecular force microscopy of cell structures and their dynamics [2]. In the case of a mechanical oscillator, the force sensitivity limit, that ultimately, arises from the classical thermal noise, is given by,

$$S_{FF}^{th} = \sqrt{4k_b T m \omega_0 / Q_m}. \quad (1)$$

Where, k_b is the Boltzmann constant, T is the temperature of the thermal environment, m , the mass of the object, ω_0 is the oscillator angular frequency and $Q_m = \omega_0 / \Gamma_0$ is the mechanical quality factor and Γ_0 is the damping factor. In recent decades, systems, such as trapped ions, have pushed the boundaries of force sensitivities down to 1×10^{-24} N/ $\sqrt{\text{Hz}}$ [3, 4]. On a more macroscopic level, cantilever devices, are able to achieve force sensitivities, reportedly down to 10^{-21} N/ $\sqrt{\text{Hz}}$ and Q_m -factors of greater than one million [5–12]. Parallel to cantilever devices, toroidal microresonators have achieved modest levels of force sensitivities $\sim 1 \times 10^{-18}$ N/ $\sqrt{\text{Hz}}$ [13]. Such toroidal microresonators have achieved Q_m -factors of up to 10^9 [14], and position sensitivities down to 1×10^{-19} m/ $\sqrt{\text{Hz}}$ [15]. These devices have a number of applications, specially as on-chip force transducers [16]. However, they are strongly limited by thermal noise from mechanical vibrations, which in such devices comes about due to mechanical coupling to the environment and equipments used to reach cryogenic temperatures.

The fundamental requirements for a good force sensor are (according to Eq. (1)); good mechanical isolation from external noise or a high Q_m -factor, low environmental temperatures and ideally low oscillation frequencies.

In levitated optomechanics, focused light is used for trapping particles in air and vacuum [17]. Levitated particles are more isolated mechanically from their environment than clamped systems and exhibit high Q_m -factors of greater than 10^6 [18–20] in translational motion, which,

in principle, are limited only by the background gas pressure and thus are predicted to reach Q_m factors $> 10^{12}$. Recently, Kuhn *et al.* [21] have reached Q_m of up to 10^{11} for a driven rotational degree of motion of a levitated nanorod at a few millibars of pressure, at room temperature. Translational motion, generally, is calculated to have force sensitivities of 1×10^{-21} N/ $\sqrt{\text{Hz}}$ [22], whilst rotational or torsional degrees of freedom of a trapped non-spherical nanoparticle are calculated to have torsional force sensitivities of 2.4×10^{-22} Nm/ $\sqrt{\text{Hz}}$ [21] to 2×10^{-29} Nm/ $\sqrt{\text{Hz}}$ [23]. As a consequence of these prospects, levitated optomechanics has attracted interest for precision measurements in electron spin resonance [24, 25], short-range forces [26], high-frequency gravitational waves [27], tests of collapse models [28, 29], the Schrödinger-Newton Eq [30] and direct dark matter detection [31].

Already, charged levitated particles have been studied in a hybrid optical-electric Paul trap [32], as well as, for demonstration of charge control in nanoparticles [3, 33]. The control of charges on nanoparticles is essential for experiments to prepare non-classical states of the motion of the particle [29, 34]. In addition, force detection at 1.63×10^{-18} N/ $\sqrt{\text{Hz}}$ in levitated nanospheres has already been demonstrated [19] by experiment.

Here, we take a detailed look at the interaction of an optically levitated dielectric particle with an external electric field as a case study for force sensing. We measure the effect of the Coulomb interaction on the motion of a single nanoparticle, at high vacuum (10^{-5} mbar) by applying a DC and an AC electric field to a metallic needle positioned near the trapped particle. These particles can carry multiple elementary electric charges (e , 1.6×10^{-19} Coulombs), and we use the Coulomb interaction to determine the number of elementary charges attached to the particle.

The charge at the needle tip, q_t , for a given applied voltage is according to Gauss's Law, $\oint_s \mathbf{E} \cdot d\mathbf{s}_t = \frac{q_t}{\epsilon_0}$, where \mathbf{s}_t is the surface of the needle tip, ϵ_0 is the vacuum permittivity, and \mathbf{E} is the electric field. The electric field at any point in a potential, V , is given by $\nabla V = \mathbf{E}$. If, we approximate the needle tip as a sphere, of radius, r_t ,

* m.rashid@soton.ac.uk

† h.ulbricht@soton.ac.uk

then $ds_t = 4\pi r_t dr$. We get,

$$\oint r_t \frac{dv}{dr} 4\pi r_t dr = 4\pi r_t V = \frac{q_t}{\epsilon_0}. \quad (2)$$

We can then combine this with the Coulomb force acting on the particle at distance, d ,

$$F_C = \frac{q_p q_t}{4\pi\epsilon_0 d^2} = \frac{q_p V r_t}{d^2}, \quad (3)$$

where, q_p is the charge on the nanoparticle. This additional force, displaces the optically trapped particle. With Eq. (3) the nanoparticle's equation of motion for general case can be written as,

$$\ddot{x}(t) + \Gamma_0 \dot{x}(t) + \frac{k}{m} x(t) = \frac{F_{th}(t)}{m} + \frac{F_c}{m} e^{i\omega_{AC} t}, \quad (4)$$

where k is the spring constant according to the optical gradient force on the particle, and F_{th} is a stochastic force originated by random process that satisfies the fluctuation-dissipation theorem [35]. The AC driving frequency, ω_{AC} , is zero when considering the DC case. d is the distance between the needle and the trapped particle, thus we can write $x(t) = d' - d$, where d' is the distance between the centre of the laser focus and needle tip, whilst $x(t)$ is the position of the particle in the trap. In the resulting quadratic equation, we can safely take x^2 as small. Considering the DC case first, we can then take the Fourier transform of Eq. (4), treating the DC contribution as,

$$\begin{aligned} F_{DC}(\omega) &= \frac{q_p V r_t}{d'} \int_{-\infty}^{\infty} \frac{e^{-i\omega t}}{d' - 2x(t)} dt \\ &= \frac{q_p V r_t}{d'} \int_{-\infty}^{\infty} \left(\frac{1}{d'} + \frac{4x(t)}{d'^2} \right) e^{-i\omega t} dt, \end{aligned} \quad (5)$$

where, we have Taylor expanded the integral in x to first order. The Cauchy principal value of the first term is zero and the right term is the same as for $x(t)$, thus,

$$\begin{aligned} F_{DC}(\omega) &= \frac{4q_p V r_t}{d'^3} \int_{-\infty}^{\infty} x(t) e^{-i\omega t} dt \\ &= \frac{4q_p V r_t}{d'^3} x(\omega) \\ &= k_{DC} x(\omega). \end{aligned} \quad (6)$$

The rest of the terms in Eq. (4) Fourier transform and once we take the squared modulus, we obtain the power spectral density (PSD) for the DC case,

$$S_{DC}(\omega) = \frac{k_b T}{2m} \frac{\Gamma_0}{((\omega' + \delta\omega)^2 - \omega^2)^2 + (\Gamma_0 + \delta\Gamma)^2 \omega^2}, \quad (7)$$

where $\omega' = \sqrt{\omega_0^2 + k_{DC}/m}$, $\delta\Gamma$ and $\delta\omega$ are the damping rate and frequency shift due to feedback cooling, respectively. This altered oscillation frequency, ω' , can be better understood as arising due to the modification of the

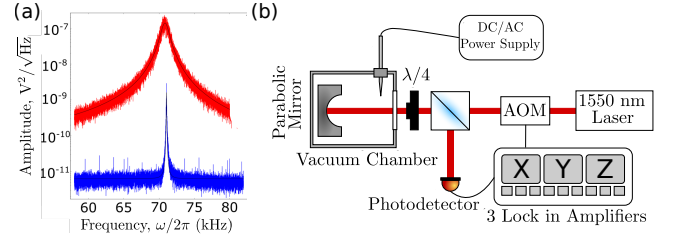


FIG. 1. Power Spectral Density and Experimental Setup: (a) Cooling the motion in z-direction of a 35 ± 2 nm diameter particle, the upper spectrum (red) is at 3 ± 0.3 mbar and the lower spectrum is at 1.6×10^{-5} mbar. This corresponds to a temperature of ~ 9 K from 300 K. (b) A mirror polished stainless steel needle is connected via a high voltage vacuum feedthrough to either a DC power supply that can output up to 20 KV or a signal generator for the AC experiments. The distance from the needle tip to the laser focus, d' , is measured to be 48.6 ± 0.8 mm. The mirror, along with the whole chamber, is earthed.

trapping stiffness experienced by the particle. By fitting Eq. (7) to the experimentally measured PSD (see Fig. 1a), the damping from background gas Γ_0 and feedback cooling $\delta\Gamma$, can be determined. These fitted parameters can then be used to work out the radius and mass of the particle, as well as, the centre-of-mass ($c.m$) temperature of the trapped particle from, $T_{cm} = \frac{T_0 \Gamma_0}{\Gamma_0 + \delta\Gamma}$.

For the AC case, $\omega_{AC} \neq 0$, and thus the AC contribution in the equation of motion in Eq. (4) has to be treated separately as:

$$F_{AC}(\omega) = \int_{-\infty}^{\infty} F_{AC}(t) e^{-i\omega t} dt \quad (8)$$

$$= \frac{F_C}{m} \int_{-\infty}^{\infty} e^{i\omega_{AC} t} e^{-i\omega t} dt \quad (9)$$

$$= \frac{F_C}{m} i\delta(w_{AC} - w). \quad (10)$$

This transform is zero everywhere other than when $w = w_{AC}$. When added with the rest of the transform of Eq. (4) we get,

$$S_{AC}(\omega) = \frac{k_b T}{2m} \frac{\Gamma_0 + |F_C|^2 \delta(w_{AC} - w)}{((\omega_0 + \delta\omega)^2 - \omega^2)^2 + (\Gamma_0 + \delta\Gamma)^2 \omega^2}. \quad (11)$$

Analysis above demonstrates that the DC contribution modifies the trap stiffness, whilst the AC driving introduces resonance enhancement of the amplitude of the oscillation signal.

In our experiments, we trap a silica nanoparticle (density, $\rho_{SiO_2} \sim 2.65$ g/cm³), in a dipole trap. The optical gradient force trap is realised using a 1550 nm laser and a high numerical aperture (N.A.) parabolic mirror to produce a diffraction limited focus. The particle's position is measured by detecting the interference between the Rayleigh scattered light by the particle and the divergent reference light with a single photodiode (as shown

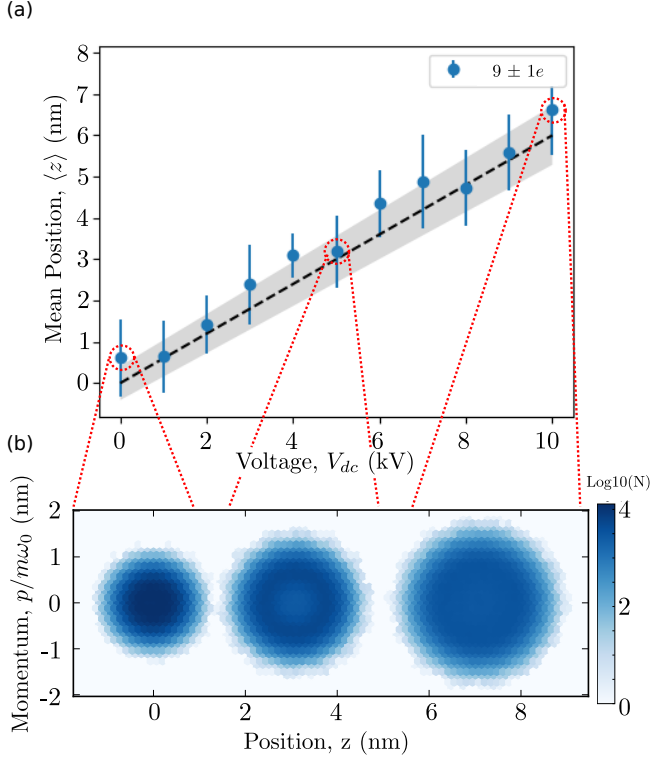


FIG. 2. **Spatial displacement:** Data shows the spatial displacement in the z -direction for a 41 ± 6 nm particle for a DC voltage of 0-10 kV applied. **(a)** Displacement of the particle's mean position at the application of different DC fields produced by the needle. **(b)** Shows the displacement of the thermal state distribution at 5 and 10 kV of 3.1 nm and 7.1 nm, respectively. Using Eq (12) gives a charge of $9 \pm 1e$. Throughout these experiments the particles $c.m$ temperature is at ~ 9 K.

in Fig. 1b). The detected signal contains three distinct frequencies for motion along x, y, z directions, which are sent to one lock-in amplifier each. The amplifiers output to an acoustic optical modulator (AOM) at twice the trap frequency with an appropriate phase shift that counters the particle motion. Thus, this parametric feedback reduces the particles $c.m$ temperature. More details can be found elsewhere [20] in regards to the trapping and cooling scheme. For both DC and AC case, we carry out the experiments at a pressure of 1.6×10^{-5} mbar and we cool the particle motion to ~ 9 K in the z -axis (see Fig.(1a)).

The needle that is used to generate the DC/AC electric field is made of polished stainless steel and has tip radius of $100 \mu\text{m}$. The distance between the trap centre to the needle, d' , is measured to be 48.6 ± 0.8 mm. To generate the DC field we connected the needle to a high power supply (Berta High Voltage Power Supply 230 series) and to generate the AC field we connect to a Signal Generator (TTi TG1010A Programmable Function Generator).

To study the effect of the DC field we use a 41 ± 6 nm

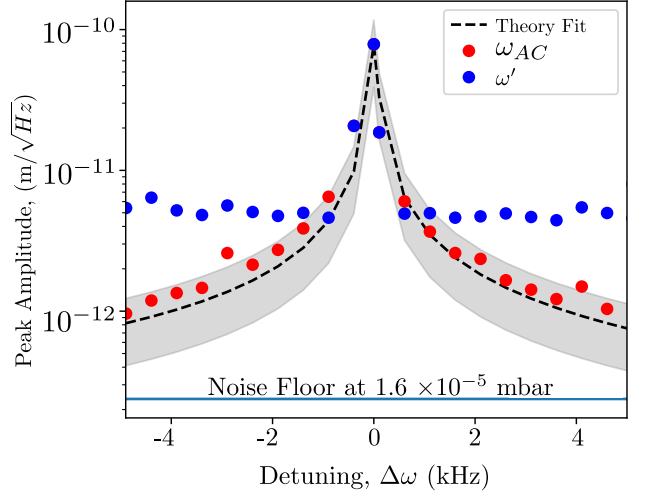


FIG. 3. **AC modulation:** Amplitude of frequency of driving AC field (in red) and levitated oscillator (in blue), are fitted to Eq. (13). The shaded region is the fitting error. With an AC force of $3.0 \pm 1.5 \times 10^{-20}$ N measured with 10 second integration and a thermal force of 3.2×10^{-20} N. The detuning, $\Delta\omega = \omega_0 - \omega_{AC}$, is swept from low to high frequencies in steps of 500 Hz to show the full spectrum response. Only the peak heights, $S_{AC}(\omega = (\omega_0))$ are shown for the given detuning.

(mass, $m = 7.6 \times 10^{-19}$ kg) silica particle. The DC field generated by the needle tip, modifies the effective potential experienced by the particle. This modification leads to both a shift in the frequency and in the mean position of the particle. The spatial displacement is shown in Fig. 2(b) and increases with increasing DC voltage. By considering that the Coulomb force is balanced with the optical gradient force, we can modify the equation of motion in Eq. (4) for the z -motion, such that $k_z z - \frac{qVr_t}{d^2} = 0$, and considering $k_z = \omega_z^2 m$ and $d = d' - z$ we get,

$$z = \frac{qVr_t}{\omega_z^2 m d'^2} \quad (12)$$

Here, z is displacement achieved in the z -direction. Fig. (2a) shows the displacement for a particle of charge of $9e \pm 1e$ and displacement of 7.1 nm for a $V_{dc} = 10$ kV. The displacement operation increases the $c.m$ temperature of the ensemble. The related increase in area of the phase-space distribution can be explained by two effects: (1) the trap becomes anharmonic because of the external DC field and (2) the increasing absolute noise on the DC voltage. Voltages greater than 10 kV result in the loss of the particle.

In the case of the AC field, it is apparent from Eq. (11) that when ω_{AC} is far from ω_0 then the PSD signal is weak but as the two converge there is a strong signal enhancement allowing much smaller forces to be detected. Fig.(3) shows both the theory and experimental plots demonstrating this enhancement effect for a particle of

radius 50 ± 6 nm. The detuning, $\Delta\omega = (\omega_0 - \omega_{AC})$, is swept in increments of 500 Hz, from off-resonance to on-resonance. By using Eq. (11), we can fit to obtain F_{AC} , which we measure, for 1 V amplitude of the AC field on-resonance, to be $3.0 \pm 1.5 \times 10^{-20}$ N integrated over 10 seconds. This approaches the achieved force sensitivity limit of 3.2×10^{-20} N/ $\sqrt{\text{Hz}}$, which is limited due to random gas collision at the pressure in the vacuum chamber. Since, we obtain F_{AC} experimentally, we can relate this to the number of charges on the particle as,

$$F_{AC} = \frac{q_p V r_t}{d^2}. \quad (13)$$

Thus, the number of elementary charges on the nanoparticle is calculated to be $4e \pm 3e$. The signal-to-noise ratio (SNR) for the AC field with resonance enhancement is 200:1, while it is 10:1 off resonance.

The limiting factor to reach even lower sensitivities than 10^{-20} N/ $\sqrt{\text{Hz}}$ can be associated to noise in the present system. This noise is a summation of detector noise, electronic noise via the feedback system, mechanical noise in the optical elements, classical thermal noise due to gas collisions and finally, the standard quantum limit (SQL). The dominating noise for the current system is the thermal noise floor according to the background gas at a pressure of 10^{-5} mbar. In addition, long term laser power drifts of approximately 1%, at timescales of hours, are introduced. This is due to polarisation change in fibre system of the laser light, which consequently causes a change in the trap frequency. This power drift predominantly effects the DC experiments, which requires the measurement of many different displacements voltages and takes many hours to carry out. On short time scales, there is electronic noise in the system due to the feedback system we use [20], specifically in the region of the trapping frequencies. The corresponding detection noise floor is shown Fig. 3. The error bars on the particle size, mass and charge are dominated by the uncertainty in the pressure readings, which is accurate to 15%.

The classical thermal noise, which has already been discussed in Eq. (1) and for levitated systems is physically realised by gas collisions, puts a strong limit on the systems sensitivity. But with modification to the current setup, i.e. for lower pressure ($\sim 10^{-9}$ mbar), with smaller particles ($r \sim 10$ nm) and trapping frequencies of ~ 100 kHz, force sensitivities down to 1×10^{-24} N/ $\sqrt{\text{Hz}}$ can be reached.

At this limit of 1×10^{-24} , it is envisaged that the standard

quantum limit (SQL) for the system would be reached. To surpass all classical noises to below this SQL it is paramount to be able to enter the quantum domain and to utilize non-classical motional features of the levitated optomechanics for force sensing. The SQL which can be written as $S_{FF}^{SQL} = \sqrt{\hbar\omega_0 m / 2\tau_F}$, where τ_F is the rate of the measurement carried out on the particle, arises due to the Heisenberg uncertainty principle [36]. For the current system the SQL is at 6×10^{-24} N/ $\sqrt{\text{Hz}}$.

In conclusion, we have measured the response of an optically levitated charged nanoparticle to a DC and an AC electric field via a needle. We have observed spatial displacement of the centre of the thermal motional state of the particle in phase space by up to 7.1 nm for an applied DC field of 10 kV. We find that by applying an AC field amplitude of 1 V on-resonance ($\omega_{AC} = \omega_0$) we are able to measure a force of 3.0×10^{-20} N with 10 second integration time. This provides an increased SNR of 200:1. The sensitivity can, in future experiments, be improved by lowering the noise floor, which is limited by the thermal noise by gas collisions at 10^{-5} mbar. We extrapolate that by optimising particle size, pressure in vacuum chamber and mechanical frequency we can reach SQL. Then, novel techniques such as squeezing in mechanical oscillators [37–39] may be used to increase for sensitivities even further. While this gives a direct perspective for the use of levitated optomechanics for force sensing applications, the system is also ideal for fundamental physics problems. The experiment can be used for a non-interferometric test of the quantum superposition principle [28]. Specifically, the continuous spontaneous localization (CSL) model [40], which gives a quantitative violation of the superposition principle, predicts a slight increase in temperature of the trapped nanoparticle. This effect, as discussed in [41, 42], can be used to set bounds on the CSL localization rate λ : the minimum excluded value of λ by the current experimental setup is $\approx 10^{-6} \text{ s}^{-1}$, which corresponds to a macroscopicity measure [43] of $\mu \approx 11$. Increasing the size of the trapped particle to $R = 300$ nm, which can be trapped by the current experimental setup, would improve the bounds on λ by two orders of magnitude.

Acknowledgments: We thank Phil Connell and Gareth Savage for expert technical help during the realisation of the experimental setup. We also like to thank Chris Timberlake, Markus Rademacher, Ashley Setter for the QPlots package and discussions. We wish to thank for funding, The Leverhulme Trust and the Foundational Questions Institute (FQXi).

-
- [1] B.P. Abbot et al, (LIGO Collaboration and Virgo), Phys. Rev. Lett. **116**, 061102 (2016).
 - [2] M. Goktas and K. G. Blank, Advanced Materials Interfaces **4**, 1600441 (2017).
 - [3] M. Gierling, P. Schneeweiss, G. Visanescu, P. Federsel, M. Häfner, D. P. Kern, T. E. Judd, A. Günther, and

- J. Fortágh, Nat. Nanotechnol. **6**, 446 (2011).
- [4] R. Maiwald, D. Leibfried, J. Britton, J. C. Bergquist, G. Leuchs, and D. J. Wineland, Nature Phys. **5**, 551 (2009).
- [5] K. Yasumura, T. Stowe, E. Chow, T. Pfafman, T. Kenny, B. Stipe, and D. Rugar, J. Microelectromech. Syst. **9**,

- 117 (2000).
- [6] H. J. Mamin and D. Rugar, Appl. Phys. Lett. **79**, 3358 (2001).
 - [7] D. Rugar, R. Budakian, H. J. Mamin, and B. W. Chui, Nature **430**, 329 (2004).
 - [8] O. Arcizet, P.-F. Cohadon, T. Briant, M. Pinard, A. Heidmann, J.-M. Mackowski, C. Michel, L. Pinard, O. François, and L. Rousseau, Phys. Rev. Lett. **97**, 133601 (2006).
 - [9] Y. Tao, J. M. Boss, B. A. Moores, C. L. Degen, and S. J. Sharp, Nat. Commun. **5**, 125424 (2014).
 - [10] M. Li, H. X. Tang, and M. L. Roukes, Nat. Nanotechnol. **2**, 114 (2007).
 - [11] J. Moser, A. Eichler, J. Güttinger, M. I. Dykman, and A. Bachtold, Nat. Nanotechnol. **9**, 1007 (2014).
 - [12] P. Weber, J. Güttinger, A. Noury, J. Vergara-Cruz, and A. Bachtold, Nat. Commun. **7** (2016).
 - [13] E. Gavartin, P. Verlot, and T. J. Kippenberg, Nat. Nanotechnol. **7**, 509 (2012).
 - [14] M. Goryachev, D. L. Creedon, E. N. Ivanov, S. Galliou, R. Bourquin, and M. E. Tobar, Appl. Phys. Lett. **100** (2012).
 - [15] A. Schliesser, G. Anetsberger, R. Rivière, O. Arcizet, and T. J. Kippenberg, New Journal of Physics **10**, 095015 (2008).
 - [16] Y.-W. Hu, Y.-F. Xiao, Y.-C. Liu, and Q. Gong, Front. Phys. **8**, 475 (2013).
 - [17] J. M. Ashkin, A. Dziedzic, Appl. Phys. Lett. **28**, 333 (1976).
 - [18] J. Gieseler, B. Deutsch, R. Quidant, and L. Novotny, Phys. Rev. Lett. **109**, 103603 (2012).
 - [19] G. Ranjit, D. P. Atherton, J. H. Stutz, M. Cunningham, and A. A. Geraci, Phys. Rev. A **91**, 051805 (2015).
 - [20] J. Vovrosh, M. Rashid, D. Hempston, J. Bateman, M. Paternostro, and H. Ulbricht, J. Opt. Soc. Am. B **34**, 1421 (2017).
 - [21] S. Kuhn, B. A. Stickler, A. Kosloff, F. Patolsky, K. Hornberger, M. Arndt, and J. Millen, arXiv:1702.07565 (2017).
 - [22] J. Gieseler, L. Novotny, and R. Quidant, Nat. Phys. **9**, 806 (2013).
 - [23] T. M. Hoang, Y. Ma, J. Ahn, J. Bang, F. Robicheaux, Z.-Q. Yin, and T. Li, Phys. Rev. Lett. **117**, 123604 (2016).
 - [24] T. M. Hoang, J. Ahn, J. Bang, and T. Li, Nat. Commun. **7**, 12250 (2016).
 - [25] L. P. Neukirch, J. Gieseler, R. Quidant, L. Novotny, and A. Nick Vamivakas, Opt. Lett. **38**, 2976 (2013).
 - [26] A. A. Geraci, S. B. Papp, and J. Kitching, Phys. Rev. Lett. **105**, 101101 (2010).
 - [27] A. Arvanitaki and A. A. Geraci, Phys. Rev. Lett. **110**, 071105 (2013).
 - [28] A. Bassi, K. Lochan, S. Satin, T. P. Singh, and H. Ulbricht, Rev. of Mod. Phys. **85**, 471 (2013).
 - [29] J. Bateman, S. Nimmrichter, K. Hornberger, and H. Ulbricht, Nat. Commun. **5** (2014).
 - [30] A. Großardt, J. Bateman, H. Ulbricht, and A. Bassi, Phys. Rev. D **93**, 096003 (2016).
 - [31] J. Bateman, I. McHardy, A. Merle, T. R. Morris, and H. Ulbricht, Sci. Rep. **5**, 8058 (2015).
 - [32] J. Millen, P. Fonseca, T. Mavrogordatos, T. Monteiro, and P. Barker, Phys. Rev. Lett. **114**, 123602 (2015).
 - [33] M. Frimmer, J. Gieseler, and L. Novotny, Phys. Rev. Lett. **117**, 163601 (2016).
 - [34] O. Romero-Isart, Phys. Rev. A **84**, 052121 (2011).
 - [35] R. Kubo, Rep. Prog. Phys. **29**, 306 (1966).
 - [36] V. Braginsky, F. Khalili, and K. Thorne, *Quantum Measurement* (Cambridge University Press, 1995).
 - [37] E. E. Wollman, C. U. Lei, A. J. Weinstein, J. Suh, A. Kronwald, F. Marquardt, A. A. Clerk, and K. C. Schwab, Science **349** (2015).
 - [38] M. Rashid, T. Tufarelli, J. Bateman, J. Vovrosh, D. Hempston, M. S. Kim, and H. Ulbricht, Phys. Rev. Lett. **117**, 273601 (2016).
 - [39] R. Riedinger, S. Hong, R. A. Norte, J. A. Slater, J. Shang, A. G. Krause, V. Anant, M. Aspelmeyer, and S. Gröblacher, Nature **530** (2016).
 - [40] G. C. Ghirardi, P. Pearle, and A. Rimini, Phys. Rev. Lett. A **42** (1990).
 - [41] A. Vinante, R. Mezzena, P. Falferi, M. Carlesso, and A. Bassi, arXiv:1611.09776 (2016).
 - [42] A. Vinante, M. Bahrani, A. Bassi, O. Usenko, G. Wijts, and T. Oosterkamp, Phys. Rev. Lett. **116**, 090402 (2016).
 - [43] S. Nimmrichter and K. Hornberger, Phys. Rev. Lett. **110**, 160403 (2013).